**1st International e-Conference
on Energies**
14 - 31 March 2014

Conference Proceedings Paper - Energies „Whither Energy Conversion? Present Trends, Current Problems and Realistic Future Solutions"

Operational Characteristics of Liquid-Piston Heat Engines

James W. Stevens [1],*, Ryan O. Kerns [2] and Jack W. Mason [2]

[1] University of Colorado at Colorado Springs, 1420 Austin Bluffs Parkway, Colorado Springs, CO, 80918; E-Mail: JStevens@UCCS.edu

[2] University of Colorado at Colorado Springs, 1420 Austin Bluffs Parkway, Colorado Springs, CO, 80918; E-Mails: rokerns@gmail.com; moonrocks101@gmail.com

* Author to whom correspondence should be addressed; E-Mail: JStevens@UCCS.edu; Tel.: +1-719-255-3581; Fax: +1-719-255-3042.

Abstract: Liquid piston Stirling engines (sometimes termed "fluidyne" engines) have been studied, proposed, and applied in a variety of energy conversion applications. They are attractive for low capital costs and simplicity of construction. This paper describes test results from a solar-powered fluidyne engine utilizing a Fresnel lens for concentrating solar energy, and from a combustion powered engine equipped with an orifice-style dynamometer for controlled loading of the engine. Temperature, pressure, and volume phasing along with indicated work and brake work are presented and discussed. The Fresnel lens provided ample power for sustained operation of the engine, and engine cycles and operational characteristics of the solar powered engine are discussed. Operating without load, the dynamic mechanical response showed no delay from the thermodynamic expansion due to temperature changes of the working fluid. The function and capacity of the orifice-style dynamometers were evaluated for testing various configurations of liquid-piston engines under load. Engine cycles and operating characteristics of the loaded engines are presented and discussed. Pressure and volume phasing was determined to not have a predominant effect on engine work output.

Keywords: fluidyne; heat engines; energy conversion; liquid piston; sustainable energy;

1. Introduction

This paper describes two separate liquid piston Stirling engine testing fixtures developed at the University of Colorado at Colorado Springs. One fixture was used to demonstrate direct solar-powered operation of a fluidyne and to explore some aspects of the operational thermodynamic cycle. One unique feature of this implementation was that sunlight was concentrated directly on the fluidyne cylinder rather than on a remote heat exchanger. The other fixture was used to place a flame powered operating engine under load with an orifice-style dynamometer and to further characterize the loaded operation of the fluidyne. These test fixtures were only intended as platforms to explore feasibility, operation, and the thermodynamic characteristics, not as practical, power producing engines.

Liquid piston Stirling engines, sometimes referred to as "fluidyne" engines, use columns of liquid to fill the role of pistons in conventional engines. Solid pistons used in conventional engines require the design, manufacture, and maintenance of sliding mechanical seals. These seals not only require tight tolerance manufacturing, they also require periodic replacement resulting in higher maintenance cost over the life of the engine. Liquid pistons do not require the manufacture or maintenance of mechanical seals which decreases overall engine costs. Furthermore, the nature of a liquid piston allows for unconventional cylinder shapes which can be useful in some applications. Fluidyne engines do not use valves or advanced timing controls for engine operation. In fact, most fluidyne engines involve very little mechanical complexity and can be manufactured with relatively few tools and simple, low-cost materials. This low capital-cost option for energy conversion makes the fluidyne appealing for certain applications in which simple manufacturing, free or low cost heat, and minimal maintenance are available [1]. While the fluidyne engine may already have a viable future in some niche applications, the device's low thermal efficiency and poor specific power currently limit its use to situations with cheap or free energy sources [2]. This includes, but is not limited to, pumping applications in developing countries or remote areas where frequent maintenance and attention may be unavailable.

Figure 1. Schmatic diagram of a fluidyne.
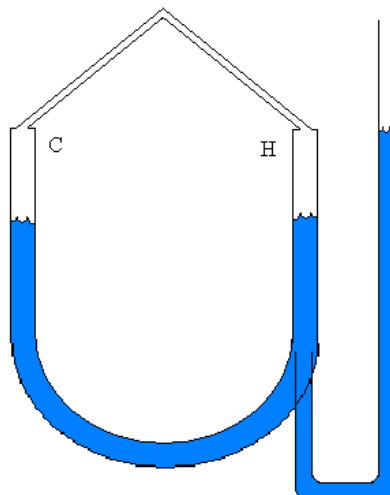
One common configuration for a fluidyne engine consists of a closed U-tube partially filled with liquid and connected at the bottom to a second tube also partially filled with liquid as shown in figure 1. The working fluid is enclosed in the sealed space above the liquid. For low-cost implementations, it is common to use water for the liquid and air for the engine working fluid. The liquid in the U-tube acts as a displacer piston which moves the working fluid from a hot side heat exchanger to a cold side heat exchanger. These heat exchangers are denoted as H and C in figure 1. As the gas in the working space shifts from side to side, it is heated and cooled causing the system pressure to increase and decrease. At the bottom of the sealed U-tube, a second liquid column is connected, and also configured in a U-tube shape. In one possible configuration, the second column (known as the output column, tuning column, or tuning line) remains open to atmospheric pressure. As the working fluid pressure rises and falls, the liquid in the output column is displaced accordingly. This oscillatory motion not only provides a means to extract work, it also provides the necessary feedback to oscillate the displacer piston in the U-tube if the fluidyne is designed correctly.

The primary advantage of fluidyne engines lies in their simplicity of construction and operation. They require little maintenance since there can be no failures of mechanical seals. They are self starting and self regulating with the application of the appropriate heat transfer interactions. Some disadvantages of the fluidyne engine include typically high losses due to fluid friction, poor heat transfer characteristics, and the introduction of phase change in the liquid columns at high temperatures [1]. Additionally, even the most recent fluidyne designs have relatively low power densities [2].

West [3] provided a comprehensive look at the history and state of the art of fluidyne engines. More recently, Fauvel et al. explored the mechanism by which the tuning line supplied feedback to the displacer piston either via hydrodynamic coupling, hydrostatic coupling, or a combination of both [2]. In that experimental study, Fauvel et al. concluded that the plain ended termination point yielded the best results with a phase lag of 49°, suggesting that the coupling mechanism from this type of fluidyne was a nearly exactly equal contribution of hydrostatic and hydrodynamic coupling [2].

The following year, 1990, Fauvel, Walker, and Reader published another article which addressed the response of both the displacer piston and tuning line to a varying system pressure [4]. Fauvel and West also published an article which corroborated experimental data from Fauvel's previous experiment with analytical data obtained from differential equations describing the piston motion [5].

A few years later, Fauvel and Yu presented another study specifically addressing the design and effectiveness of a barrel-type fluidyne [6]. This study differed from Fauvel's previous work by focusing more on a practical design of a fluidyne instead of scientific understanding. In 2004, an article published by Orda and Mahkamov described an empirical study of different water pumps, collecting efficiency and pumping capacity data [7]. The study involved three different prototypes; the first employed the use of a heated element in a concentric cylinder design, the second utilized flat-plate solar collectors in a U-tube design, and the third design improved the second design with a more compact form. All three fluidyne models contained a solid displacer piston in between the hot and cold side columns which was attached to a spring to aid in cycling the liquid back and forth. While Orda and Mahkamov only presented experimental data from their own fluidyne designs, their study

presented physical data of solar-heated fluidyne engines which can operate under the varying conditions of solar collection and pumping needs.

A study published by Slavin, Bakos, and Finnikov concentrated on the development of fluidyne engines for medium power electricity generation [8]. The group conducted a computer simulation which analyzed a more complex fluidyne that contained multiple valves and chambers. Another study by Özdemir and Özgüc [9] attempted to formulate a mathematical model based on hydrodynamic and thermodynamic equations and compared that model to an actual experiment. Similar to the Slavin et al. study, the model was built on hydrodynamic and thermodynamic equations, except for the additional interfacial conditions that occur in a wet fluidyne (evaporation and condensation). The simulation data supported the experimental prototype, however the authors did comment that the weakness of the model was the modeling of the interfacial mechanisms.

An article published in 2009 reflected on the benefits of using a liquid piston Stirling engine as a mobile hydraulic power supply option [10]. The authors mostly discussed the efficiency benefits of the Stirling engine and the cost benefits associated with using liquid pistons in them. The qualitative discussion included the application of this engine to automotive powerplants, robotics, construction equipment, irrigation pumping in developing nations and the Stirling engine's potential use as a heat pump.

2. Results and Discussion

2.1. System Descriptions

The first test fixture was intended to explore the feasibility and operating characteristics of a direct solar power liquid piston engine. It was to be powered by the sun using a 50" by 37" Fresnel lens. The displacer piston was constructed of 1" diameter piping. The tuning column consisted of ½" tubing. The framed Fresnel lens was mounted on a wooden stand. The lens pivoted on support arms that were the same length as the focal length of the lens. This design allowed the fluidyne to remain stationary on the stand and simultaneously allowed the focal point to remain positioned on the hot side of the heat exchanger, even as the lens was raised and lowered to face the sun. Figures 2 and 3 show the fluidyne engine and lens stand respectively.

The second test fixture was built to explore the use of an orifice-type dynamometer to impose an external load on the flame powered fluidyne. The main body of the displacer piston was made 5.1 cm diameter copper pipe and each piston was 35.6 cm long. The working space was constructed of 1.9 cm diameter copper tubing with two 90° connections to make an approximate "U" shape. The tuning column diameter was 3.8 cm and the tuning column length was 2.9 m. Figure 4 shows the fluidyne for the second test fixture. The orifice-type dynamometers were placed in the tuning column well above the reach of the oscillating liquid. Three different loads were tested using orifice diameters of 6.4 mm, 4.8 mm, and 3.2 mm corresponding to small, medium and large loads on the engine, respectively, as air above the tuning column had to be forced through the orifices.

Both test fixtures were instrumented with thermocouples, a differential pressure transducer in the working space, and a water level measurement device in the tuning column. In addition, the second

fixture included a second pressure transducer in the tuning column, and a second level measurement device in the cold side of the displacer.
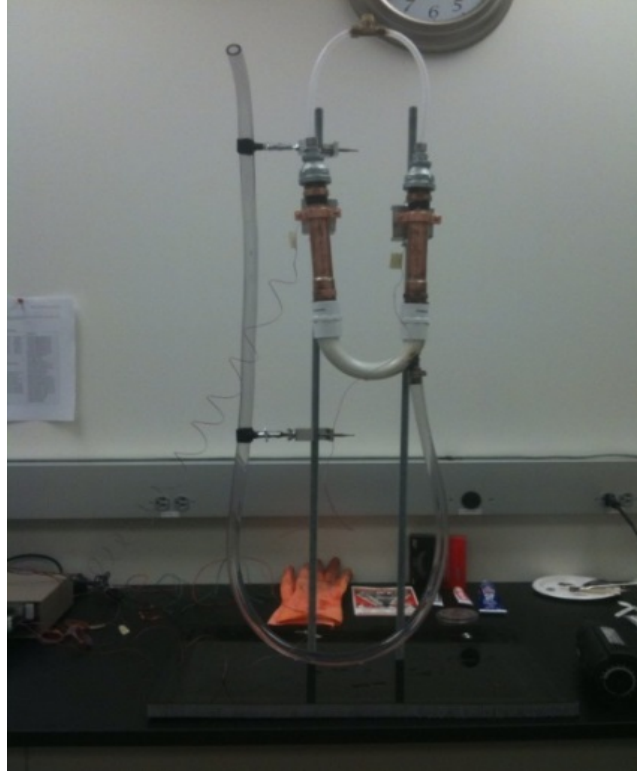
Figure 2. Solar powered fluidyne engine.

Figure 3. Fresnel lens and mounting stand.

Figure 4. Combustion powered fluidyne engine with orifice-style dynamometer.

2.2. Results

Figure 5 shows about 20 seconds of temperature data from a single test of the first (solar powered) test fixture. During this segment, the temperature fluctuations on the hot side were about 4 deg C, and the temperature fluctuations on the cold side were approximately 12 deg C. As expected, the temperature fluctuations from the two thermocouples are out of phase with one another.

This engine was operated without any external load for this phase of testing. Therefore, the indicated cycle work is only overcoming internal friction and other losses. Figure 6 shows actual working space pressure and volume measurements for four cycles plotted with different symbols in order to make the details of the cycle work more visible. Also overlaid in figure 6, shown with a heavier black line and no symbols is a simple P-V prediction based on sinusoidal motion of the displacer piston and output piston and scaled to fit the measured volume and pressure fluctuations. The overall agreement is forced by the scaling, however, the scaling allows a comparison between the shapes of the measured cycle and the idealized P-V shape. It can be seen that the measured data has a more concave shape during compression and a more convex shape during expansion than the idealized cycle.

Figure 7 demonstrates, for the first six cycles of the data presented earlier (for clarity) a plot of the temperature difference between the hot side and the cold side, overlaid onto a plot of the measured pressure. It can be seen that the temperature difference fluctuations are exactly in phase with the pressure fluctuations. This confirms that the dynamic mechanical response of this unloaded engine closely tracks the thermodynamic expansion of the working fluid.

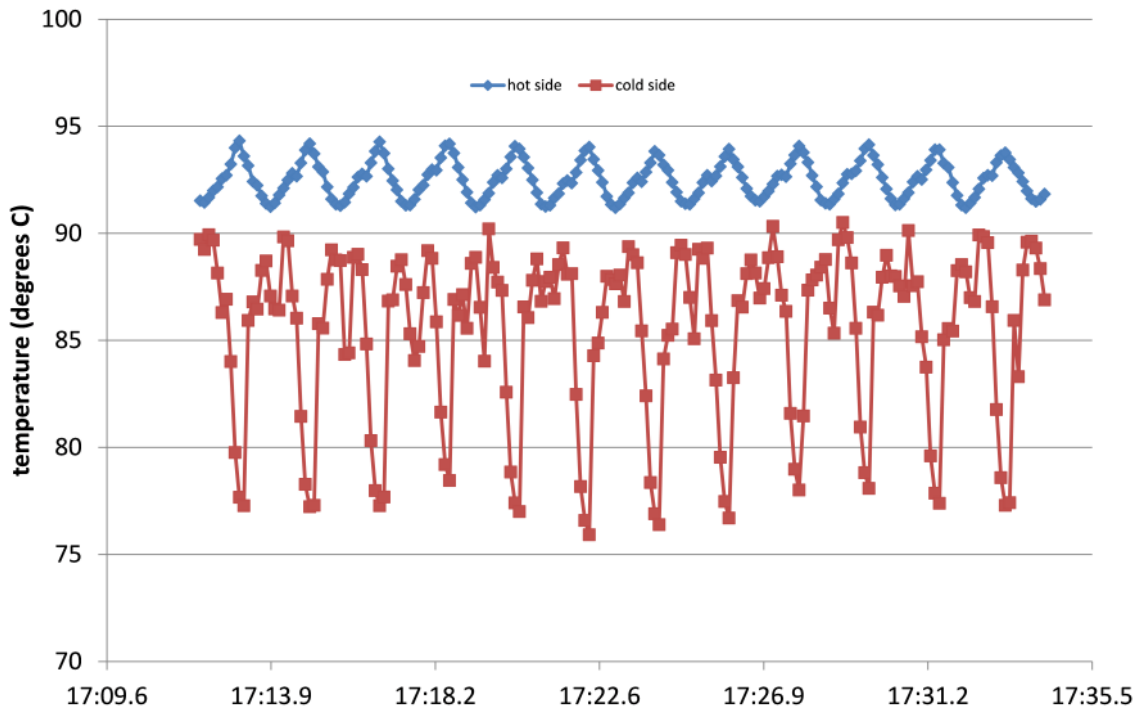**Figure 5.** Hot and cold side temperature fluctuations from the solar powered fluidyne.

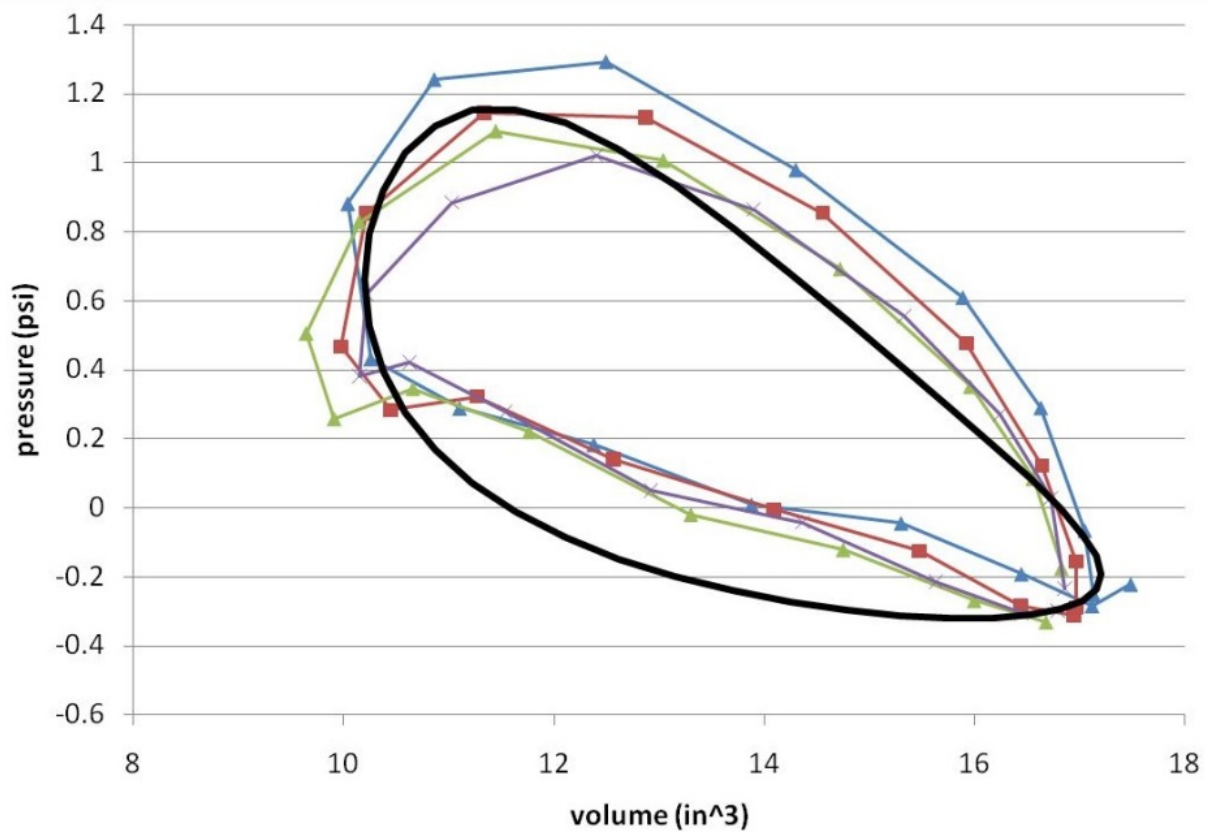**Figure 6.** Pressure vs. volume plot along with a scaled, idealized cycle.

Figure 7. Pressure and temperature data from the solar powered fluidyne.
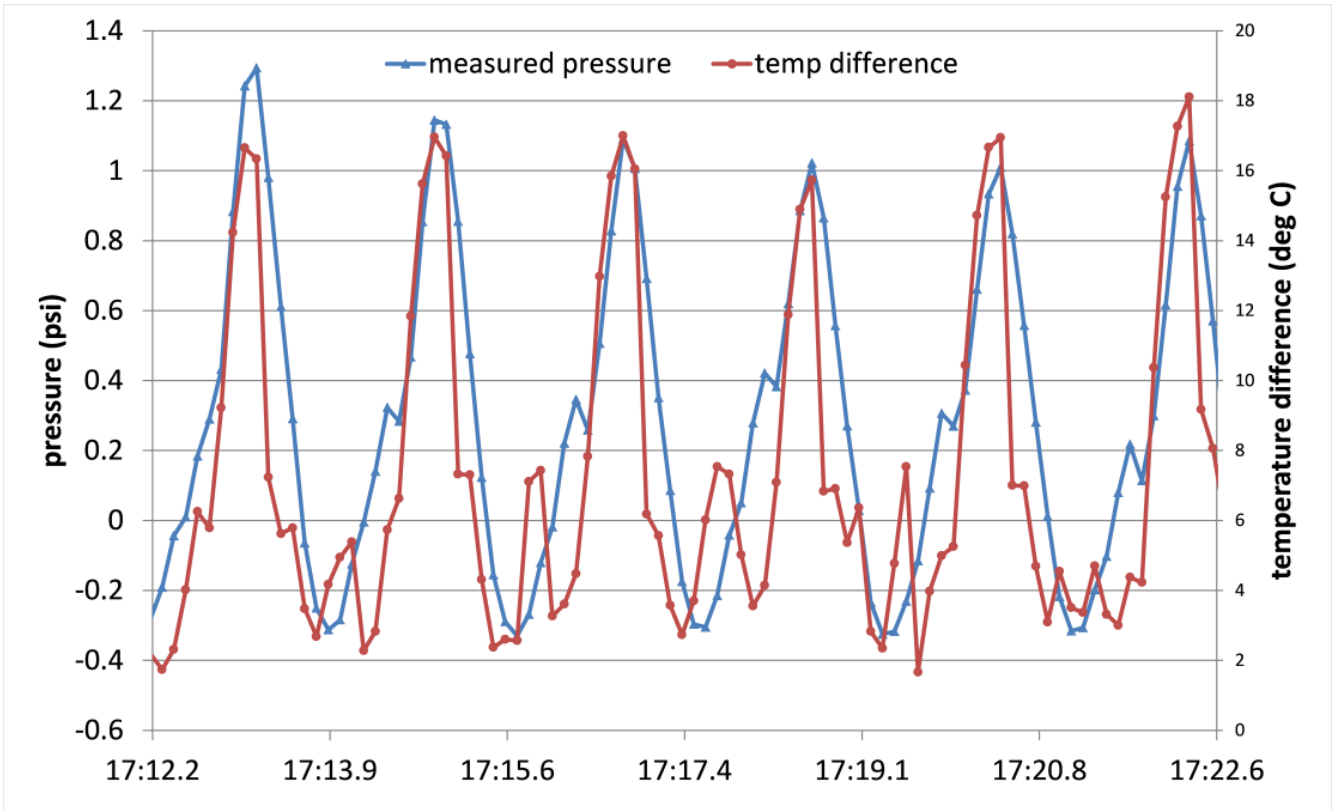

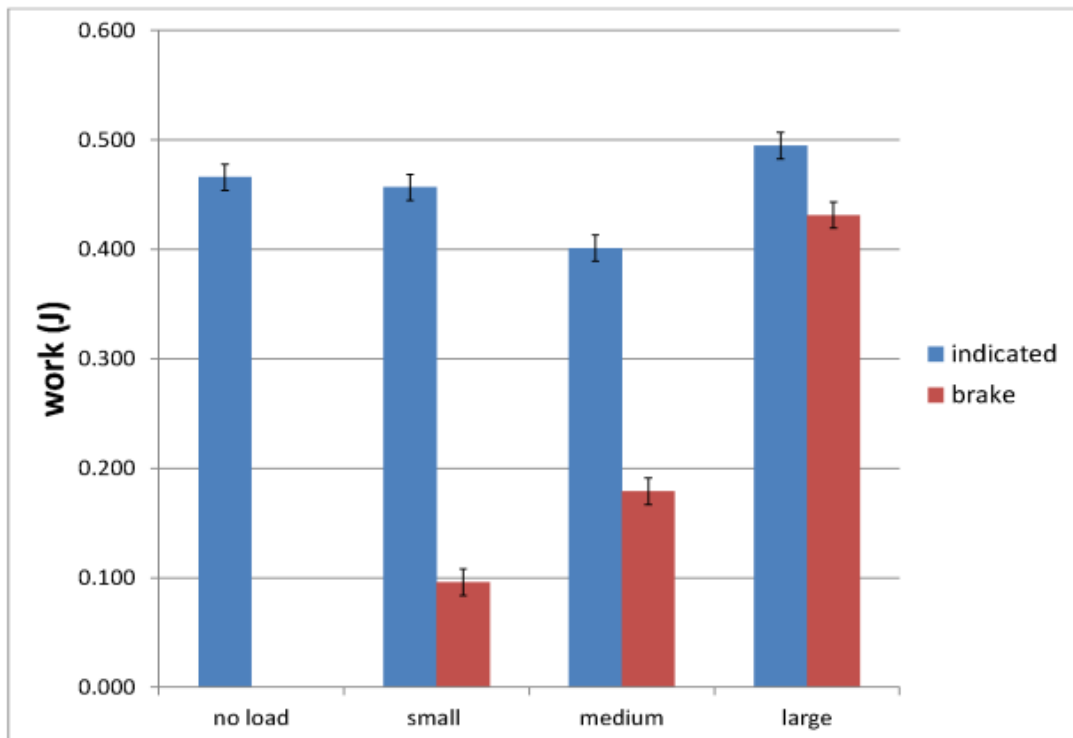**Figure 8.** Indicated and brake work output per cycle from the second test fixture.

Figure 8 demonstrates data available from the second test fixture equipped with an orifice-type dynamometer. Indicated work was calculated by integrating the pressure and volume change inside the working space, and brake work was determined by integrating the pressure and volume change above the tuning column. Figure 8 shows the average brake work and indicated work per cycle for the three different loading cases, and the indicated work for the no-load case. For the highest load, the brake work approaches 87% of the indicated work with no significant degradation in engine operation. Eventually, an external load that was too large would be expected to stall the engine, but that case was not explored in this work.

Figure 9 shows the phasing between the working space pressure and the working space volume for the three loading cases and the no-load case. For the unloaded case the pressure fluctuations are 173 degrees ahead of the volume fluctuations, and increasing load pushes the phase difference down by almost 40 degrees from the no-load case to the most heavily loaded case.

Figure 10 shows the same kind of phasing information as figure 9, except for the tuning column rather than the working space. Thus, figure 10 shows phasing information for brake work, while figure 9 pertains to indicated work. In this case, the pressure and volume are closer to 90 degrees out of phase, with the loading again reducing the phase difference, albeit by a smaller amount, about 15 degrees.

Figure 11 demonstrates a qualitative comparison of the effect of phasing alone on the expected work output (either indicated or brake) of the engine. This figure was prepared using equal scales to emphasize the relative shape of the P-V plot as a function of phase angle, and does not present actual measured pressure and volume data as in figure 6. A phase difference of 90 degrees between the system pressure and the system volume leads to, in these comparative coordinates, a circular P-V plot which would maximize the available work for a given range of volumes and pressures. Figure 11 shows comparative shapes for the measured phase angles from figure 9. It can be seen that the indicated work phasing for the no-load case of 173 degrees leads to an elongated P-V plot. The loading pushes the indicated work toward a more favorable phasing, although that effect is not evident in the cycle work results plotted in figure 8. Similarly, the increased loading pushes the brake work away from the optimum phasing of 90 degrees, (lower, this time) but the opposite trend is apparent for brake work in figure 8. Clearly, the P-V phasing is not the dominant effect in the total work output of the engine.

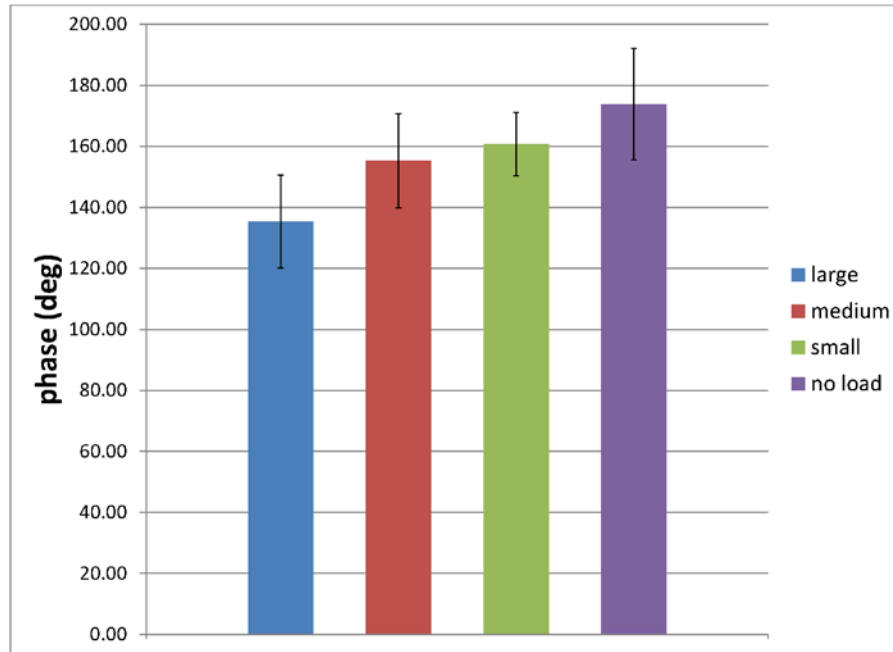**Figure 9.** Pressure and volume phasing for the working space of the dynamometer equipped test fixture.

Figure 10. Pressure and volume phasing for the tuning column of the dynamometer equipped test fixture.
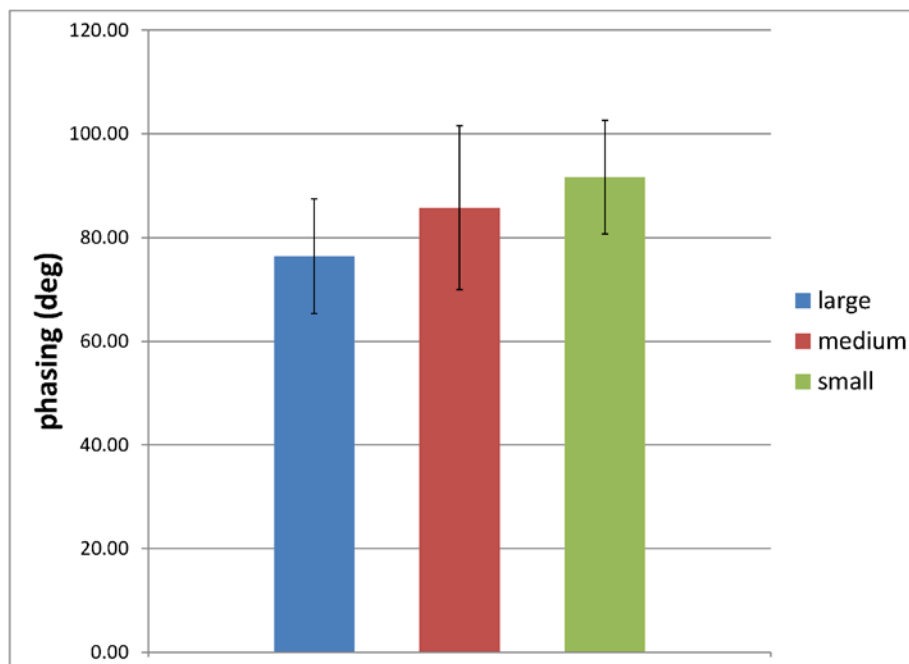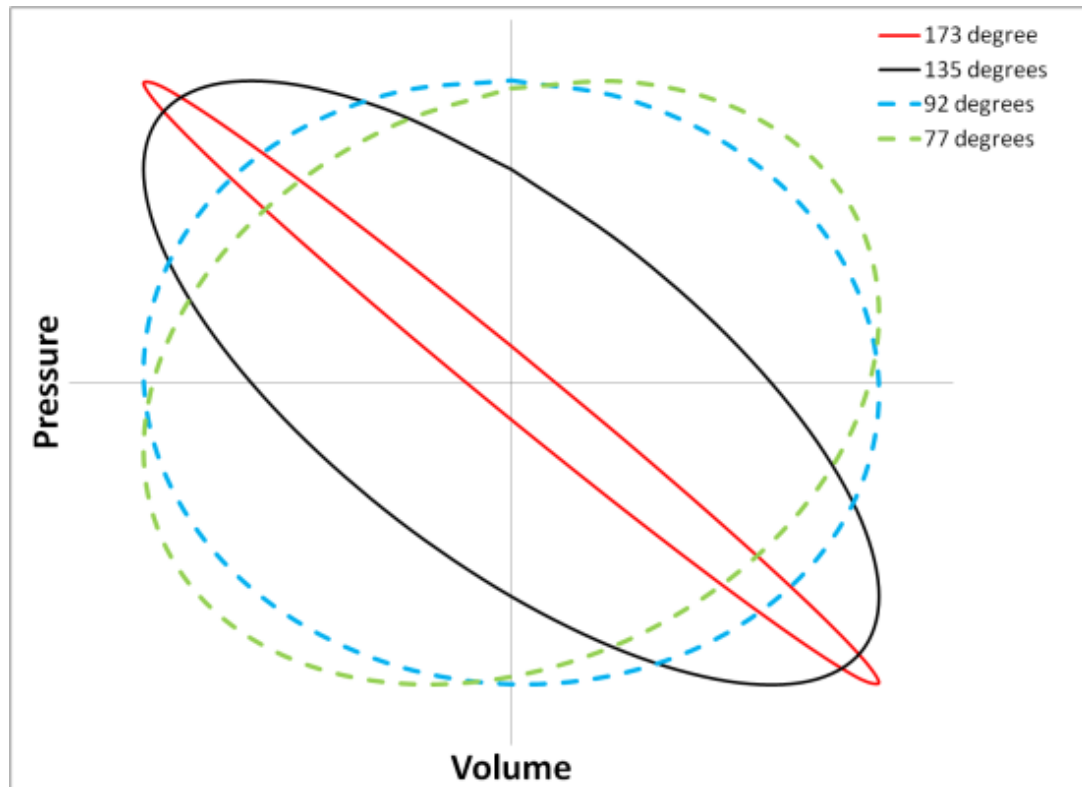
Figure 11. Qualitative comparison of P-V shapes as a function of phase angle.

3. Conclusions

An instrumented solar-powered fluidyne test fixture demonstrated consistent and repeatable operation. A Fresnel lens focused sunlight directly on the hot cylinder of the fluidyne with no intermediate heat exchanger and was able to provide ample energy to power the fluidyne. Indicated work of the engine was collected with pressure and volume measurements. Since the engine was unloaded, this work only overcame frictional losses. The shape of the indicated work in a cycle was compared to the shape of a simple thermodynamic expansion and compression in a Stirling cycle with the same volume and pressure range imposed. It was found that the dynamic mechanical response of the unloaded engine showed no delay from the thermodynamic expansion due to temperature changes. A second test fixture consisted of a flame-powered instrumented fluidyne equipped with an orifice-type dynamometer. This fixture demonstrated the capacity to impose an independent external load on an operating engine. Only a loading regime well away from engine stall was explored. It was demonstrated that while external loading affected the P-V phasing of the engine, the phasing alone was not the dominant effect in either the indicated work or the brake work produced by the engine under load.

Conflicts of Interest

The authors declare no conflict of interest.

References

1. Stevens, J.W., "Low Capital Cost Renewable Energy Conversion With Liquid Piston Stirling Engines" *Proceedings of ASME 2010 4t h International Conference on Energy Sustainability*, **2010**, Phoenix, AZ , ES2010-90129.
2. Fauvel, O. R., Reader, G. and Walker, G, "Tuning Line Excitation of Displacer Motion in a Fluidyne", *Proceedings of the 24th IECEC*, Aug 6-11, **1989**, Vol. 5, p. 2271.
3. West, Colin D., *Liquid Piston Stirling Engines.* Van Nostrand Reinhold: New York, USA, 1983.
4. Fauvel, O. R., Walker, G. and Reader, G., "Excitation of a Fluidyne Tuning Line", *Proceedings of the 25th IECEC*, Aug 12-17, **1990**, Vol. 5, p. 315.
5. Fauvel, O. R. and West, C. D., "Excitation of Displacer Motion in a Fluidyne", *Proceedings of the 25th IECEC*, Aug 6-11, **1990**, Vol. 5, pp. 336-341.
6. Fauvel, O. R. and Yu, L., "Displacer Design and Testing For a Barrel Fluidyne", *Proceedings of the 29th IECEC*, Aug 7-11, **1994**,Vol. 4, pp. 1950-1953.
7. Orda, E. and Mahkamov, J., "Developement of 'Low-tech' Solar Thermal Water Pumps for Use in Developing Countries", *Journal of Solar Energy Engineering*, **2004**, Vol. 126, pp. 768-773.
8. Slavin, V. S., Bakos, G. C. and Finnikov, K. A., "Conversion of thermal energy into electricity via a water pump operating in a Stirling Engine Cycle", *Applied Energy*, **2009**, Vol. 86, pp. 1162-1169.
9. Özdemir, M and Özgüc, A. F., "A simple mathematical model to analyse a fluidyne heat machine", *Proceedings of the Institution of Mechanical Engineers, Part A: Journal of Power and Energy*, **2003**, Vol. 217, pp. 91-100.
10. Van de Ven, James D., "Mobile hydraulic power supply: Liquid piston Stirling engine pump", *Renewable Energy*, **2009**,Vol. 34, pp. 2317-2322.